A Combined Density Functional Theory and Coupled Cluster Method Investigation of the Structural Properties and Stabilities of Radical CH_2CP and Its Isomers

Hai-tao Yu,[†,‡] Ming-xia Li,[‡] and Ke-li Han*[,†]

State Key Laboratory of Molecular Reaction Dynamics, Dalian Institute of Chemical Physics, Chinese Academy of Sciences, Dalian 116023, China, School of Chemistry and Materials Science, Heilongjiang University, Harbin 150080, China

Received: July 19, 2005; In Final Form: December 11, 2005

The doublet potential energy surface of radical system [C_2, H_2, P] is investigated at the UB3LYP/6-311++G(d,p) and UCCSD(T)/6-311++G(2df,2p) (single-point) levels. Eight chainlike and three-membered ring structures are located as energy minima connected by 10 interconversion transition states. At the final UCCSD(T)/6-311++G(2df,2p)//UB3LYP/6-311++G(d,p) level with zero-point vibrational energy correction, species CH_2CP is found to be thermodynamically the most stable isomer followed by HCCPH, H−*c*CPC−H, *c*PCC−H(H), H−*c*CCP−H, *cis*-CC(H)PH, *trans*-CC(H)PH, and $CCPH_2$ at 11.01, 12.57, 40.07, 43.63, 50.25, 56.82, and 65.36 kcal/mol, respectively. The computed results indicate that the chainlike isomers CH_2CP and HCCPH and cyclic radical H−cCPC−H possess considerable kinetic stability at extra low pressures and temperatures. Interestingly, radical $CCPH_2$, whose energy is the highest in all predicted CH_2CP isomers, can be also regarded as a kinetically stable species with the smallest isomerization barrier of 22.26 kcal/mol at extra low pressures and temperatures. Therefore, considering higher kinetic stability, in addition to the microwave spectroscopy characterized isomer CH_2CP in previous experiments, the species HCCPH, H−cCPC−H, and $CCPH_2$ should be considered as excellent candidates for possible experimental observation. Furthermore, the structural nature of stable radical isomers is discussed based on bonding characteristics, single electron spin distribution, and comparison with their analogues.

1. Introduction

Recently, phosphorus-containing molecules have been extensively studied in a variety of fields, such as organic and inorganic synthesis, organometallic chemistry, and interstellar chemistry,[1−4] due to the multivalence feature of the phosphorus atom. But the knowledge of radicals with multiple carbon−phosphorus bond is very limited. Up to now, only a few small molecule radicals with carbon−phosphorus multiple bonds have been experimentally investigated, such as the diatomic species CP[5−7] and tetratomic radicals HCCP[8] and CH_2P.[9] The CP radical is one of two phosphorus-bearing molecules that have been identified in interstellar space.[10] More recently, another species with carbon−phosphorus multiple bond, CH_2CP, which is the derivative of the methyl radical resulting from substitution of one of the hydrogen atoms by a CP group, is investigated by Ahmad[11] and Ozeki.[12] Ahmad et al.[11] experimentally studied the rotational, centrifugal distortion, and spin-rotation coupling constants of CH_2CP radical by laboratory submillimeter-wave spectroscopy. Simultaneously, the molecule proved theoretically to be planar, being similar to its nitrogen analogue CH_2CN.[13,14] Ozeki and co-workers[12] have observed the hyperfine resolved rotational spectrum of the CH_2CP radical in the $\tilde{X}^2B_1$ ground electronic state using a Fourier transform microwave spectrometer. The experimental results also suggested that the CH_2CP radical forms an allenic structure rather than a phosphoryl form. To our knowledge, besides the two pioneering experimental investigations[11,12] noticed above, the relative stability or geometrical structures of the various possible isomers of compounds CH_2CP are not known. Then, a detailed knowledge about the structure, bonding, stability, and isomerization properties of various CH_2CP isomers is very desirable and helpful for understanding the nature of CH_2CP system. Therefore, we here report a detailed computational study on the reaction and isomerization potential energy surface (PES) of a [C_2, H_2, P] system with an attempt to predict potential isomers that are kinetically stable and some structural information on relevant species.

2. Computational Methods

All calculation procedures are implemented in the Gaussian 98 program package [15] running on the SGI/Origin300 server. Since the investigated molecule is an open shell system, the computed wave function is not necessarily the eigenfunction of the spin operator $\langle s^2 \rangle$, but it contains contaminating terms from higher spin eigenfunctions. Considering this disadvantage, the UB3LYP treatment[16−18] has been chosen here because of the desire to obtain better spin density values. The UB3LYP/6-311++G(d,p)-computed results indicate that the spin contamination from higher spin eigenfunctions was found to be quite small. The harmonic vibrational frequencies and intensities of all species, which are used to characterize the nature of all stationary points, are calculated by means of the UB3LYP method in conjunction with the 6-311++G(d,p) basis set, using the geometrical parameters calculated at the UB3LYP/6-311G++(d,p) theory level. To improve the energies, single-point calculations are performed at the UCCSD(T)/6-311++G(2df,2p) level[19,20] employing the UB3LYP/6-311G++(d,p)-optimized geometries. Unless otherwise specified, the energies

* Corresponding author. E-mail: yuht@263.net.cn.
† Dalian Institute of Chemical Physics.
‡ Heilongjiang University.

10.1021/jp0539977 CCC: $33.50
Published on Web 01/28/2006

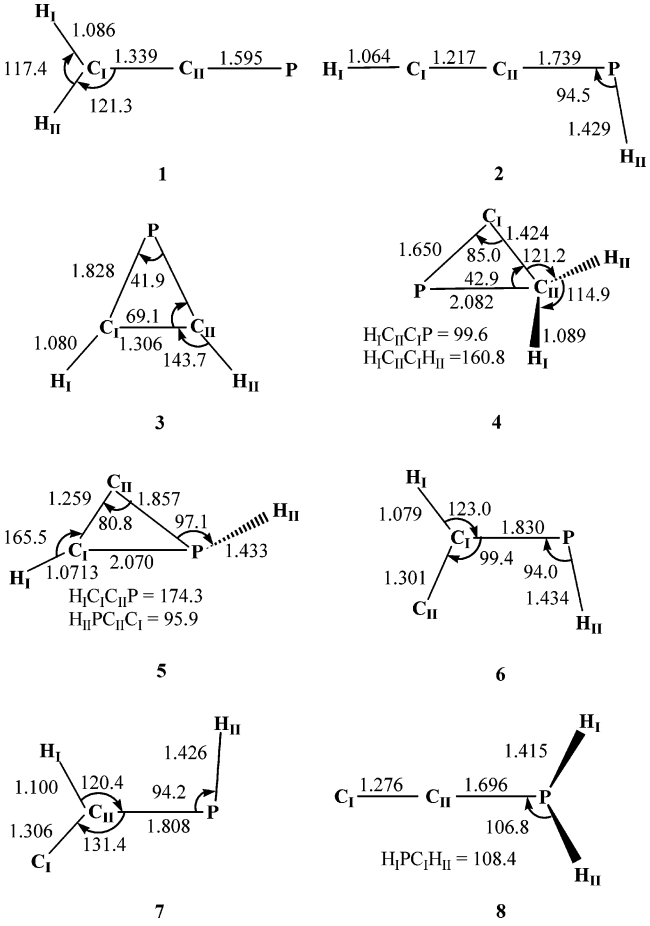

Figure 1. Calculated geometries of [C_2, H_2, P] isomers at the UB3LYP/6-311++G(d,p) level of theory. Bond lengths are in angstroms and bond angles in degrees.

at the UCCSD(T)/6-311++G(2df,2p)//UB3LYP/6-311G++-(d,p) level with UB3LYP/6-311G++(d,p) zero point energy corrections are used in the present study. To confirm whether these obtained transition states connect the right reactants and products, intrinsic reaction coordinate (IRC) calculations[21,22] are performed at the UB3LYP/6-311G++(d,p) level of theory. Mulliken spin density analysis is utilized to discuss the bonding nature of some relevant isomers.

Furthermore, the radical stabilization energy (RSE) is used to predict some structural features of relevant species. The RSE is taken to be the difference of bond dissociation energies (BDEs) between BDE_H, the C−Y bond dissociation energy for X = H, and BDE_X, the C−Y bond dissociation energy for $X \neq H$. The BDE is described as

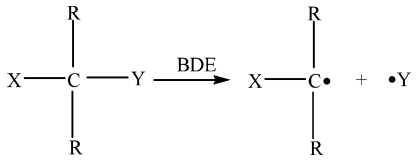

3. Results and Discussion

Eight CH_2CP structural forms are optimized at the UB3LYP/6-311++G(d,p) level, and their structures are given in Figure 1. To examine the interrelation between the CH_2CP isomers, 10 interconversion transition states, whose geometries are shown in Figure 2, are obtained at the same theory level. For later discussions easier, the Arabic number ***m*** is used to denote various isomers, and the symbol **TS*m*/*n*** to denote the transition

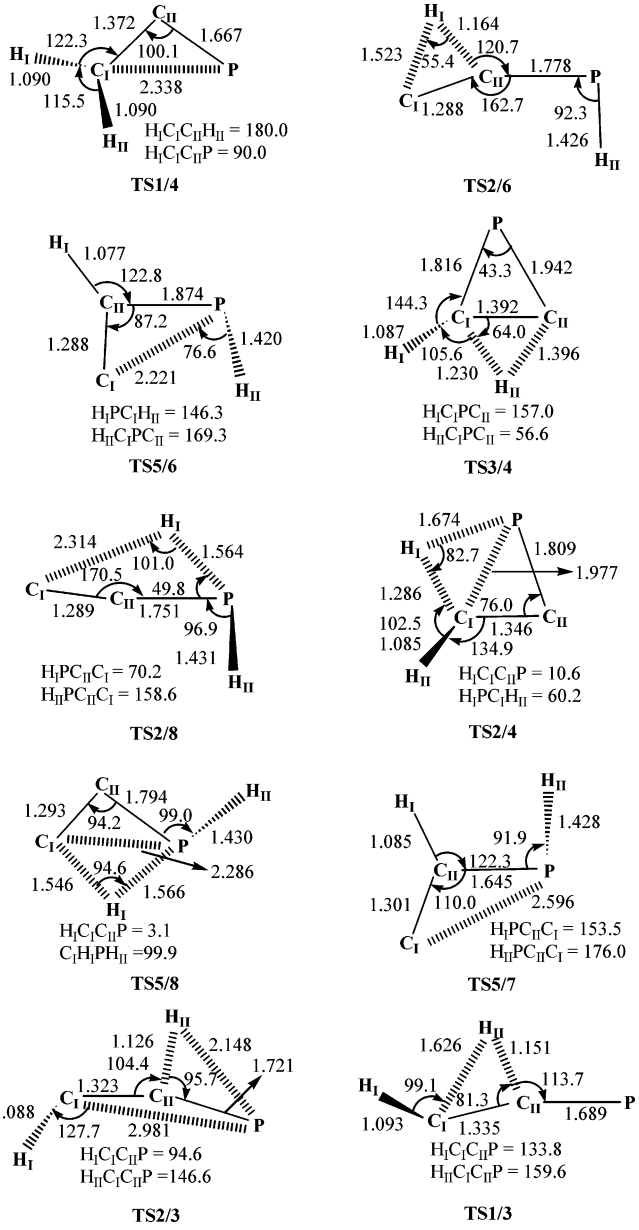

Figure 2. Calculated transition state geometries of [C_2, H_2, P] system at the UB3LYP/6-311++G(d,p) level of theory. Bond lengths are in angstroms and bond angles in degrees.

state between the isomers ***m*** and ***n***. By means of the located isomers and corresponding transition states, a schematic potential energy surface is plotted in Figure 3. For simplicity, the structural details of the obtained 10 transition states are omitted in Figure 3. The harmonic vibrational frequencies, infrared intensities, dipole moments, and rotational constants of the CH_2CP species are listed in Table 1, while the total and relative energies with zero-point vibrational energy (ZPVE) corrections of the isomers, transition states, and dissociation products are summarized in Table 2.

3.1. Isomers. Frequency calculations show that the eight species presented in Figure 1 are all local minima with all real vibrational frequencies. The located species CH_2CP (**1**), HCCPH (**2**), CC(H)PH (**6** and **7**), and $CCPH_2$ (**8**) have chainlike or branching chainlike structures. Isomer **1** has C_{2v} symmetry with a $^2B_1$ electronic state, while the isomer **8** has C_s symmetry with a $^2A'$ electronic state, whereas species **2**, **6**, and **7** all have C_s symmetry with a $^2A''$ electronic state. Note that both isomers **6** and **7** have the CC(H)PH structure, but they have *cis*-CCPH

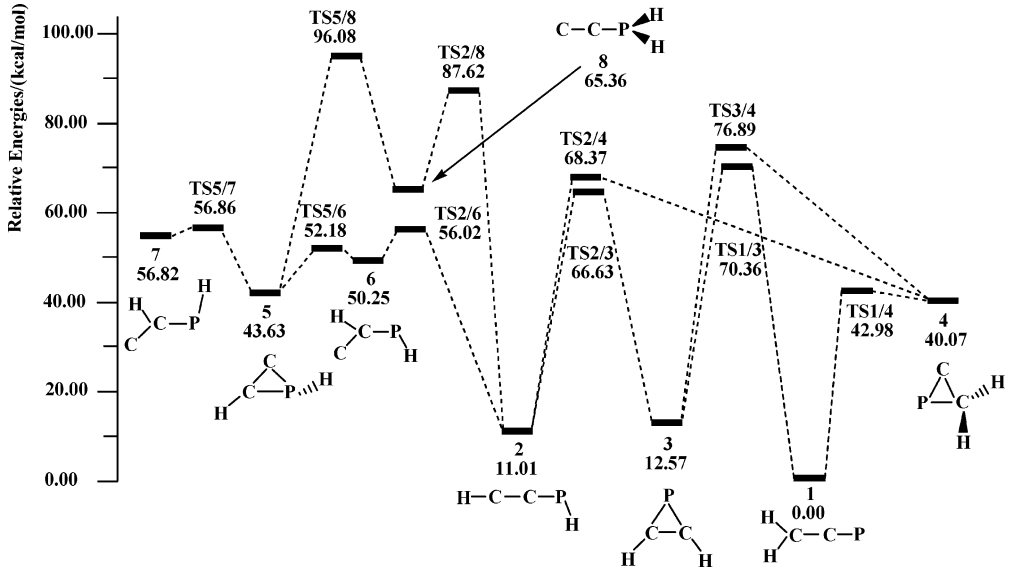

Figure 3. Schematic reaction potential energy surface of [C_2, H_2, P] system at the UCCSD(T)/6-311++G(2df,2p)//UB3LYP/6-311++G(d,p) level with zero-point vibrational energy correction.

TABLE 1: Harmonic Vibrational Frequencies (cm^{-1}), Infrared Intensities (km/mol) (in Parentheses), Dipole Moment (Debye), and Rotational Constants (GHz) of Optimized [C_2, H_2, P] Isomers at the UB3LYP/6-311++G(d,p) Level of Theory

species	frequency (infrared intensity)	dipole moment	rotational constant
CH_2CP, **1**	321.6 (15.2), 337.4 (13.1), 814.6 (44.1), 828.5 (0.1), 989.8 (3.9), 1409.9 (0.1), 1570.2 (20.2), 3111.9 (0.1), 3192.7 (0.1)	1.2381	291.0484, 5.4734, 5.3724
HCCPH, **2**	270.8 (7.7), 280.4 (7.7), 619.2 (41.5), 638.9 (51.2), 665.9 (22.3), 916.1 (46.6), 2023.9 (10.3), 2339.7 (73.2), 3460.5 (65.0)	1.0084	255.5388, 5.3910, 5.2796
H−*c*CPC−H, **3**	592.0 (19.1), 634.1 (76.7), 723.6 (8.7), 893.8 (0.0), 907.1 (1.3), 1008.7 (55.0), 1622.7 (8.2), 3213.5 (0.9), 3252.3 (0.1)	1.6737	33.9148, 11.3809, 8.5213
*c*PCC−H(H), **4**	383.1 (10.1), 669.1 (24.7), 966.1 (65.1), 1002.3 (0.0), 1036.9 (18.1), 1195.4 (16.5), 1486.6 (2.3), 3072.2 (7.7), 3150.3 (2.8)	1.4903	36.9821, 10.1120, 8.3881
H−*c*CCP−H, **5**	233.8 (2.5), 485.8 (10.8), 648.4 (60.0), 649.4 (49.5), 818.3 (33.8), 926.6 (26.6), 1783.5 (17.5), 2301.8 (127.8), 3359.6 (49.8)	1.8115	38.2781, 9.4726, 8.0626
cis-CC(H)PH, **6**	260.1 (1.4), 369.3 (2.9), 659.2 (17.6), 714.3 (52.7), 715.4 (0.3), 998.9 (36.3) 1633.0 (77.0), 2324.8 (18.5), 3257.1 (29.2)	2.0172	40.4870, 8.4147, 6.9667
trans-CC(H)PH, **7**	159.3 (15.7), 250.7 (0.0), 572.6 (30.4), 646.5 (24.9), 802.0 (4.0), 944.2 (21.3), 1619.9 (146.5), 2368.0 (81.2), 3025.8 (40.4)	2.5837	71.9729, 6.2158, 5.7216
$CCPH_2$, **8**	168.6 (43.5), 196.6 (0.7), 558.5 (55.0), 757.6 (13.0), 829.5 (23.8), 1103.3 (106.1), 1844.7 (57.0), 2410.0 (37.0), 2434.2 (17.4)	4.8407	140.5094, 5.7048, 5.6244

and *trans*-CCPH backbone chains, respectively. The species H−*c*CPC−H (**3**), *c*PCC−(H)H (**4**), and H−*c*CCP−H (**5**) are CCP three-membered ring forms. Isomer **3** is in the electronic state of $^2B_1$ with C_{2v} symmetry and two exocyclic CH bonding. Structure **4** with $^2A'$ state has C_s symmetry and two exocyclic CH bonding, while isomer **5** has C_1 symmetry with exocyclic CH and PH bonding.

From Table 2, we can obtain the energetic ordering of the located CH_2CP minimum isomers at the single-point UCCSD-(T)/6-311++G(2df,2p) level. Generally, the species with lower total energy has higher thermodynamical stability. Thus, at the UCCSD(T)/6-311++G(2df,2p)//UB3LYP/6-311++G(d,p) level with zero-point energy correction, the thermodynamical stability order of these isomers is **1** (0.00) > **2** (11.01) > **3** (12.57) > **4** (40.07) > **5** (43.63) > **6** (50.25) > **7** (56.82) > **8** (65.36). The values in parentheses are relative energies in kcal/mol with reference to the lowest-lying isomer **1**. It is very clear that the chainlike isomer **1** is thermodynamically the most stable species.

3.2. Isomerization and Kinetic Stability of Isomers. In addition to the thermodynamical stability, a discussion of the kinetic stability of various CH_2CP isomers may be of more interest. In present paper, we only consider kinetic stability respect to monomolecular reactions, which correspond with the experimental conditions of extra low pressures and temperatures. The smallest isomerization barrier may usually govern the kinetic stability of an isomer. To provide further insight into the stability of various isomers, we also considered the related dissociation pathways of species to fragments. Since the relative energies of the dissociation products are rather high (more than 70 kcal/mol at the UCCSD(T)//B3LYP level) as shown in Table 2, we can clearly know that the isomerization processes govern the kinetic stability of CH_2CP isomers rather than the dissociation ones.

As shown in Figures 2 and 3, some CH_2CP isomers can interconvert via simple isomerization processes, such as direct H-shift (**2** → **6**, **2** → **8**, and **3** → **4**) and simple ring-open processes (**4** → **1**, **5** → **6**, and **5** → **7**). Some species can interconvert via more complex processes, such as the conversions **3** → **1**, **3** → **2**, **4** → **2**, and **5** → **8**, which include H-shift and ring-open processes simultaneously.

In fact, we can briefly discuss the kinetic stability of these obtained isomers in terms of the smallest barrier of isomerization from them. From Figure 3, we can obtain the kinetic stability order of the CH_2CP isomers as **3** (54.06 for **3** → **2**) > **2** (45.01 for **2** → **6**) > **1** (42.98 for **1** → **4**) > **8** (22.26 for **8** → **2**) > **5** (8.55 for **5** → **6**) > **4** (2.91 for **4** → **1**) > **6** (1.93 for **6** → **5**) > **7** (0.04 for **7** → **5**). Notice that the values in parentheses denote the smallest isomerization barriers of CH_2CP isomers in kcal/

TABLE 2: Total Energies (TE, au), Zero-Point Energies (ZPE, au/particle), Single-Point Energies (SPE, au), and Relative Energies (RE, kcal/mol) of Isomers, Fragments, and Transition States of the [C_2, H_2, P] System

species	TE[a]	SPE[b]	ZPE[c]	RE[d]
CH_2CP, **1**	−418.73315	−418.07677	0.02865	0.00
HCCPH, **2**	−418.70953	−418.05612	0.02555	11.01
H−cCPC−H, **3**	−418.70838	−418.05736	0.02927	12.57
c-PCC−H_2, **4**	−418.66367	−418.01380	0.02953	40.07
H−cCCP−H, **5**	−418.65546	−418.00413	0.02553	43.63
cis-CC(H)PH, **6**	−418.64621	−417.99294	0.02491	50.25
trans-CC(H)PH, **7**	−418.63691	−417.98130	0.02373	56.82
$CCPH_2$, **8**	−418.62563	−417.96744	0.02347	65.36
$CC(^1\Sigma_g) + PH_2(^2B_1)$	−418.43649	−417.82418	0.01759	151.56
$CC(^2\Pi) + PH_2(^2B_1)$	−418.47302	−417.82101	0.01718	153.29
$PH(^3\Sigma) + CCH(^2A')$	−418.53555	−417.88541	0.01861	113.78
$CH(^2\Pi) + HCP(^1\Sigma)$	−418.52806	−417.88224	0.02041	116.90
$HCCP(^3\Sigma) + H(^2S)$	−418.59499	−417.94214	0.01758	77.54
H−cCCP($^1A'$) + $H(^2S)$	−418.56502	−417.92014	0.01807	91.65
trans-HPCC($^1A'$) + $H(^2S)$	−418.52643	−417.87671	0.01434	116.56
$HC \equiv CH(^1\Sigma_g^+) + P(^2D)$	−418.57614	−417.93121	0.02705	90.34
$HC \equiv CH(^1\Sigma_g^+) + P(^4S)$	−418.63818	−417.99450	0.02705	50.63
TS1/4	−418.65952	−418.00797	0.02834	42.98
TS5/6	−418.64152	−417.98936	0.02440	52.18
TS2/6	−418.63491	−417.98088	0.02203	56.02
TS1/3	−418.62002	−417.95900	0.02301	70.36
TS2/4	−418.61338	−417.96283	0.02368	68.37
TS3/4	−418.60047	−417.94981	0.02422	76.89
TS2/8	−418.58445	−417.92872	0.02023	87.62
TS5/8	−418.56721	−417.91553	0.02053	96.08
T5/7	−418.63564	−417.98136	0.02386	56.86
T2/3	−418.61583	−417.96520	0.02327	66.63

[a] At the UB3LYP/6-311++G(d,p) level of theory. [b] At the UCCSD(T)/6-311++G(2df,2p) level using the UB3LYP/6-311++G(d,p)-optimized geometries. [c] At the UB3LYP/6-311++G(d,p) level of theory. [d] At the single-point UCCSD(T)/6-311++G(2df,2p)//UB3LYP/6-311++G(d,p) level with zero-point energy correction, and relative energy of thermodynamically the most stable radical CH_2CP is set to zero.

mol at the UCCSD(T)/6-311++G(2df,2p)//UB3LYP/6-311++G(d,p) level of theory with zero-point vibrational energy correction. Therefore, the three isomers **1**, **2**, and **3** have considerable kinetic stability (more than 40 kcal/mol) and may be observable in experiments provided that accurate precursors and experimental conditions are available.

It should to be noted that the rearrangement reaction from **2** to **1** occurs theoretically via a cyclic intermediate **3** and two relevant transition states rather than a direct one-step process since the direct H-migration transition state from **2** to **1** has not been located despite of a lot of work performed. The resemblance was mentioned in a previous study about the nitrogen analogues for the transition from HCCNH to H_2CCN predicted by Balucani and co-workers.[23]

For isomer **8**, which lies 65.36 kcal/mol above the isomer **1** and is thermodynamically the most unstable species in all of the located isomers, its kinetic stability is very surprising. The reaction barrier 22.26 kcal/mol for **8** → **2**, which is much smaller than these for **3** → **2**, **2** → **6**, and **1** → **4**, is still considerable. The computational results suggest it to be stable enough to be observable at some experimental conditions with normal temperature. Considering the higher thermodynamical instability for **8**, we took a long time to search possible transition states connecting it and other isomers or dissociation fragments, including the direct H-shift transition state from **8** to **6** that is expected to have a lower barrier. But, unfortunately, all failed. Therefore, we carried out some additional computations for the direct H-shift transition process using potential energy surface scanning technology. The computed results are plotted in Figure 4. In the computations, we gradually decrease the angle H_IPC_{II} θ, and other bond lengths and angles are full optimized. The

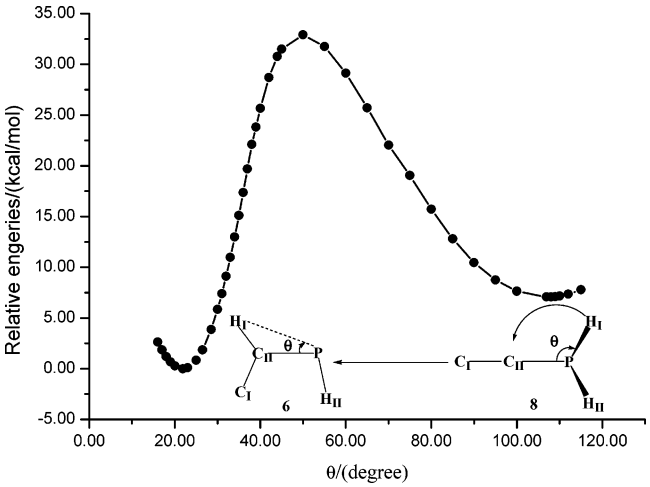

Figure 4. H-shift channel between isomers **6** and **8** obtained by potential energy surface scanning technology at the UB3LYP/6-311++G(d,p) level of theory.

potential energy curve indicates that the transition process from **8** to **6** has a reaction barrier of 25.85 kcal/mol, which is higher than that of **8** → **2** via transition state **TS2/8**. So, all computed results suggest isomer **8** to be a kinetically stable species corresponding with the monomolecular reaction. We hope that the isomer can be given some evidence of existence by experimental chemists in future. Furthermore, we will do some structural descriptions supporting the theoretical prediction in the next section as well.

The remaining isomers **4**, **5**, **6**, and **7** have much lower kinetic stabilities (barriers less than 10.0 kcal/mol), so they may be of little interest as observable species either in the laboratory or in space.

3.3. Structural Properties of the Relevant Species. From section 3.2, we can know that, among various [C_2, H_2, P] isomeric forms, only four species, CH_2CP (**1**), HCCPH (**2**), H−*c*CPC−H (**3**), and $CCPH_2$ (**8**), possess considerable kinetic stability and may be observable in the laboratory at extralow pressures and temperatures. Now, let us analyze their structural and bonding properties. For parallel comparison on the C−P, C═P, C≡P, C−C, C═C, and C≡C bonding, additional UB3LYP/6-311++G(d,p) calculations (with frequency confirmation as stationary points) are carried out for the structures of model systems H_3C-PH_2, $H_2C{=}PH$, HCP, H_3C-CH_3, $H_2C{=}CH_2$, and HCCH. In the following, the bond length comparisons are made with the above UB3LYP/6-311++G(d,p) results.

3.3.1. Isomer CH_2CP. The lowest-energy isomer, CH_2CP (**1**), is in the ground electronic state of $^2B_1$ and has C_{2v} symmetry with two equivalent carbon−hydrogen bonds. The calculated carbon−carbon bond length is 1.339 Å, which is slightly shorter than the value 1.342 Å at the CCSD(T) level in the equilibrium structure of CH_2CP predicted by Ahmad and co-workers.[11] It can be regarded as a slightly weak double bond, which is in agreement with Ahmad's prediction,[11] because the distances of normal C−C single and C═C double bonds are 1.530 and 1.329 Å in the species ethane (CH_3-CH_3) and ethylene ($CH_2{=}CH_2$), respectively. The carbon−phosphorus (1.595 Å) bond length in isomer **1** is slightly longer than the corresponding value (1.5889 Å) in Ahmad's calculation,[11] and it lies between the typical C═P double bond length of 1.671 Å in CH_2PH and CP triple bond length of 1.540 Å in HCP. Therefore, the CP bond can be considered as a stronger double bond or a weak triple bond, being well consistent with the microwave spectrum results given by Ozeki and co-workers.[12]

TABLE 3: Calculated CC and CX Bond Lengths (Å), Spin Densities on Relevant Atoms, and Radical Stabilization Energies (RSEs, kcal/mol) of CH_2CX (X = N, P, As) Molecules

	bond lengths[a]		spin densities[a]		RSEs[b]		
species	r_{CC}	r_{CX}	β-C	X	B3LYP[c]	CCSD[d]	primary structures
H_2CCN	1.379	1.169	0.91	0.42	10.49	6.70	$H_2C-C\equiv N$
H_2CCP	1.339	1.595	0.66	0.72	23.81	19.00	$H_2C=C=P$
H_2CCAs	1.343	1.715	0.54	0.82	29.64	24.93	$H_2C=C=As$

[a] At the UB3LYP/6-311++G(d,p) level. [b] CH_4 used as a reference molecule. [c] At the UB3LYP/6-311++G(d,p) level with zero-point energy correction. [d] At the UCCSD(T)/6-311++G(2df,2p)//UB3LYP/6-311++G(d,p) level with zero-point energy correction.

In fact, we can also understand the structural feature of CH_2CP from its electronic structure:

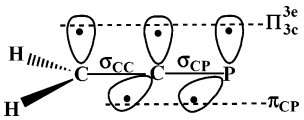

In the electronic structure, there is a out-of-plane 3c−3e bond residing on the CCP chain. The unpaired electron occupies the out-of-plane p orbital, agreeing with previous experimental results.[12] The results of stronger carbon−phosphorus double bond and weaker carbon−carbon double bond can be considered to come of electron transfer from a single electron on β-C and located electrons on the out-of-plane carbon−phosphorus π bond to the carbon−carbon bond which has lower electron density.

Again, the calculated spin density distribution (0.66, −0.31, and 0.72 e for β-C, α-C, and P, respectively) indicates that the single electron is mainly located at the P and β-C atoms. This is in good agreement with the experimental prediction.[12] Therefore, we can describe the molecular structure of CH_2CP (**1**) as two resonant forms, $H_2C=C=P^{\bullet}$ and $H_2C^{\bullet}-C\equiv\ddot{P}$.

From the estimated spin densities on the phosphorus and β-carbon atoms from the hyperfine coupling constants, Ozeki regarded the molecular structure of CH_2CP as a linear combination of two canonical configurations,[12] namely, phosphoallenic (C=P double bond nature) and phosphoryl (CP triple bond nature) forms with an approximate weight of one to one or forms as a species including a weak double bond and a strong double bond. On the basis of the calculated structural nature in present work, we suggest that in isomer **1** the component of $H_2C=C=P^{\bullet}$ structure should be slightly more than that of $H_2C^{\bullet}-C\equiv\ddot{P}$ form, which is in good accordance with the experimental results of 0.54 and 0.67 spin single electron distribution ratio on β-carbon and phosphorus atoms,[12] respectively. Thus, although isomer CH_2CP (**1**) can be considered to form from the molecule $H_3C-C\equiv P$ via the removal of a hydrogen atom of methyl or from the methyl via substitution of one of the hydrogen atoms by a CP group, which can directly lead to the formation of the $H_2C^{\bullet}-C\equiv P$ structure, we preferably deem it more possible to engender from species $HPCCH_2$, in which the CP and CC bond distances (1.647 and 1.305 Å, respectively) are closer to the corresponding bond lengths in CH_2CP than those in species CH_3CP, via the cleavage of C−H bond and the loss of H atom.

For more exact interpretation for the structural properties of CH_2CP (**1**), some additional computations were performed for CH_2CN and CH_2CAs, the nitric and arsenic analogues of CH_2CP radical, at the UB3LYP/6-311++G(d,p) level of theory. The computed results are collected in Table 3. For CH_2CN, its CN bond length (1.169 Å) is very close to the normal CN triple bond (1.150 Å in HCN), while its CC bond can be regarded as a stronger single bond because of a 1.379 Å bond distance. Furthermore, spin density analysis indicates that the main unpaired electron is located on the β-C and nigrogen atoms with 0.91 and 0.42 e, respectively, which is consonant with the corresponding experimental spin density distribution of 0.95 and 0.26 e on the two atoms.[12] Thus, species CH_2CN can be described as $H_2\dot{C}-C\equiv\ddot{N}$ form rather than $H_2C=C=\dot{N}$ structure, or we can say that CH_2CN has a π-delocalized structure with some amount of ketenemine character, being in excellent agreement with previous experimental and theoretical prediction.[12,14] For CH_2CAs molecule, its CC bond, which is slightly longer than that in CH_2CP by only 0.004 Å, shows obvious double bonding feature. The calculated results also indicate that the spin density (0.82 e) on the arsenic atom is higher than these on phosphorus (0.72 e) and nitrogen (0.42 e) atoms, as shown in Table 3. Therefore, the single electron distribution of the radical mainly locates on the arsenic atom. Hereby, we can describe the CH_2CAs radical as $H_2C=C=\dot{A}s$ and $H_2\dot{C}-C\equiv As$ structures, where the former has more weight.

TABLE 4: Calculated CC BDEs in CH_2CX (X = N, P, As) Molecules

species	products	G2	G2(MP2)	exp
CH_2-CN	$CH_2(^3B_1) + CN(^2\Sigma)$	136.64	136.77	138.22[a]
CH_2-CP	$CH_2(^3B_1) + CP(^2\Sigma)$	140.62	140.73	
CH_2-CAs	$CH_2(^3B_1) + CAs(^2\Sigma)$	139.75	139.31	

[a] The enthalpies of formation of CH_2 and CN were taken from the following reference: Chase, M. W., Jr. *J. Phys. Chem.* Ref. Data, Monograph 9, 1998, 1−1951. Those for CH_2CN were taken from the following reference: Holmes, J. L.; Mayer, P. M. *J. Phys. Chem.* **1995**, *99*, 1366.

On the basis of the computed results, we notice that the CC bond lengths in CH_2CN, CH_2CP, and CH_2CAs do not always decrease with an increase of atomic number from N to As, e.g., 1.379, 1.339, and 1.343 Å, respectively. In the computations, we can find that the bond distance order is in accordance with the corresponding BDE values, shown in Table 4. The computed results for the BDE of CH_2-CN bond are 136.64 and 136.77 kcal/mol at the G2[24] and G2(MP2)[25] levels, respectively, which are very close to the value, 138.22 kcal/mol, estimated from the corresponding experimental enthalpies of formation of relevant species. For CH_2-CP and CH_2-CAs, no sufficient experimental data for forecasting their BDEs are available. The results indicate that the increasing order of carbon−carbon BDEs is accordant with the decreasing order of carbon−carbon bond lengths in the molecules CH_2CN, CH_2CP, and CH_2CAs.

In fact, we can also have an insight into the structural characteristics by analyzing the single electron delocalization effect by means of every molecular RSE, which can efficiently reflect the effect of substituent upon the stability of radical center. Generally, the species with lower RSE has lower electron delocalization effect from the radical center. The bond dissociation energy of substituted species is employed to calculate the effect of substituent on radical stability in present study. The calculated results with zero-point vibrational energy correction are collected in Table 3. Obviously, the ordering of the stabilization energy on radical center is $RSE_{CH_2CN} < RSE_{CH_2CP} < RSE_{CH_2CAs}$, which indicates that the delocalization effect of unpaired electron on the β-C atom of CH_2CN is minimal, and maximal for the β-C atom of CH_2CAs. The increasing tendency of delocalization effect on going from CH_2CN to CH_2CAs obtained from RSEs is in excellent agreement with the direct theoretical results from B3LYP computations about electron spin density distribution shown in Table 3.

TABLE 5: Predicted Relevant Bond Lengths (Å), Spin Densities, and Structures of HCCXH (X = N, P, and As) and C−H BDEs (kcal/mol) of the Parent Molecule CH_2CXH

species		HCCNH	HCCPH	HCCAsH
bond lengths[a]	r_{CC}	1.240	1.217	1.214
	r_{CX}	1.268	1.739	1.873
spin densities[a]	β−C	0.70	0.41	0.26
	X	0.57	0.87	0.92
primary structures		HC═C═NH	HC≡C−PH	HC≡C−AsH
C−H BDEs	B3LYP[b]	96.78	76.95	71.14
	CCSD[c]	96.50	74.38	68.02

[a] At the UB3LYP/6-311++G(d,p) level. [b] At the UB3LYP/6-311++G(d,p) level with zero-point energy correction. [c] At the UCCSD(T)/6-311++G(2df,2p)//UB3LYP/6-311++G(d,p) level with zero-point energy correction.

3.3.2. Isomer HCCPH. The $^2A''$ state structure HCCPH **2** possesses a 1.217 Å CC bond, which should be regarded as an intermediate between CC double bond and CC triple bond by comparison with the corresponding bond distances in ethylene (C═C double bond, 1.329 Å) and acetylene (CC triple bond, 1.199 Å). Its calculated CP bond length (1.739 Å) is about 0.139 Å shorter than the normal C−P single bond length of 1.878 Å and is about 0.068 Å longer than the normal C═P double bond distance of 1.671 Å. This indicates that the CP bond possesses some certain π-bonding characteristics. Thus, species **2** can be best viewed as a resonance structure between H−C≡C−Ṗ−H and H−Ċ═C═P−H. The calculated results indicate that the distribution of spin density is 0.41, −0.23, and 0.87 e on the β-C, α-C, and P atoms, respectively, which suggests a larger contribution from the C≡C triple bond configuration. Accordingly, of the two extreme resonance structures H−C≡C−Ṗ−H and H−Ċ═C═P−H, the former has more weight. Therefore, it is more possible to produce radical **2** from the molecule $HCCPH_2$ via the loss of a hydrogen atom connecting with the phosphorus atom rather than from the species H_2CCPH via the removal of a hydrogen atom from the β-C atom. Of course, the HCCPH radical can also be considered as a derivative of the HCCX molecule resulting from substitution of the X atom or group by a PH group, which is a possible experimental synthesis pathway for the radical.

For better comprehension for the structural peculiarities of HCCPH, we have carried out some additional computations for nitrogen and arsenic analogues of HCCPH, HCCNH ($^2A''$) and HCCAsH ($^2A''$). The structural discrepancies can be reflected in the diminishing CC bond lengths and spin densities of β-C atoms and the gradually increased spin densities of X atoms (X = N, P, and As) from HCCNH to HCCAsH, as presented in Table 5. The species HCCNH, which has well characterized by both experimental and theoretical methods,[23,26,27] possesses a CC bond distance of 1.240 Å, which justly suggests it to be an intermediate between CC double bond and CC triple bond. Moreover, in view of a small difference of spin density distribution, 0.57 e on the nitrogen atom and 0.70 e on the β-C atom, free radical HCCNH exhibiting a stronger delocalization effect should be described as an intermediate structure between two extreme resonance forms HĊ═C═NH and HC≡C−Ṅ H, in which the former has slightly more weight. Consequently, we would rather call it a diolefin-like structure than the propargylene-like form employed by Balucani and co-workers.[23] From the CC bond length as shown in Table 5, one can easily find that the CC bond in HCCAsH is closer to a CC triple bond than those in HCCPH and HCCNH. Moreover, the 0.92 e unpaired electron spin density on the arsenic atom, which suggests HCCAsH to be a HC≡C−ȦsH structure and to exhibit a weak delocalization nature, indicates that the CC triple bond feature is more obvious in HCCAsH than in HCCPH and HCCNH.

TABLE 6: Predicted Relevant Bond Lengths (Å), Bond Angles (deg), and Spin Densities of Three-membered Ring Species H−cCXC−H (X = N, P, and As)

species		H−*c*CNC−H	H−*c*CPC−H	H−*c*CAsC−H
bond lengths	r_{CC}	1.292	1.306	1.301
	r_{CX}	1.443	1.828	1.964
bond angles	∠CXC	53.2	41.9	38.7
spin densities	C	0.10	0.03	0.02
	X	0.81	0.94	0.97

As is known widely, electron delocalization can effectively stabilize a radical, and then, we can also estimate the single electron delocalization effect from the C−H bond dissociation energies of the parent molecules H_2CCXH (X = N, P, and As), or we may also say that the substituent effects on the bond dissociation energies are often discussed on the basis of the stabilities of radicals. The computational results are shown in Table 5. Generally, the stronger the single electron delocalization effect of the formed radical is, the smaller the bond dissociation energy of parent molecule. The diminishing C−H bond dissociation energies from parent molecules H_2CCNH to H_2CCAsH clearly reflect the computed single electron delocalization effect, being excellent agreement with the computed spin density distribution of X atoms shown in Table 5.

3.3.3. Isomer H−cCPC−H. Isomer H−*c*CPC−H **3** with C_{2v} symmetry and $^1B_2$ electronic state has a CPC three-membered ring with two identical exocyclic C−H bonds. The CP bond length 1.828 Å in species **3** suggests that the CP bond has a slightly strong single bond feature by comparing it with the CP single bond length of 1.878 Å in CH_3-PH_2. The CC (1.306 Å) bond length is very close to the typical double bond length (1.329 Å) in ethylene. The spin density distribution (0.94 and 0.03 e for P and C, respectively) indicates that the single electron mainly resides at the phosphorus atom, and no obvious delocalization exists on the CCP ring, being in accord with the exhibition in the isovalent cyclopropenyl and cyclic azirinyl radicals.[28−31] As a result, species **3** can be written, despite of the existence of a nominal CP double bonding property, as the structure

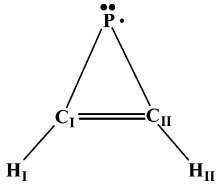

To make use of some accessional computations, presented in Table 6, and drawn molecular orbital pictures (Figure 5, parts a and b) occupied by unpaired electron using the Molden program,[32] one can easily find that the localization effect of single electron dominates the structural nature of H−*c*CPC−H and its nitrogen and arsenic analogues, H−*c*CNC−H and H−*c*CAsC−H, and almost no delocalization effect is noticed. This can also be reflected from the perfect π_{CC} orbital shown in Figure 5c. In the three radicals, the CC bond lengths differ from one another by less than 0.014 Å, indicating nearly uniform double bonding character, described schematically in Figure 5a as an feckly unaided π bond with nominal p component of the X atom, which is in good agreement with the regularity reflected from nearly the same spin density values at the three X atoms shown in Table 6. Some computational results about the composition of several important orbitals using the natural

TABLE 7: Components of X−C Bond Orbital (σ_{XC}) and Orbitals O_{sp^2} and P_z Occupied by Lone-paired Electrons and by Single Electron, Respectively

bond orbital	O_{sp^2}		σ_{XC}		P_z
atom	X		X	C	X
atom orbital	s	p			p
H−cCNC−H	69.9%	30.1%	56.6% (s, 15.4%; p, 84.6%)	43.4% (s, 21.3%; *p*, 78.7%)	100%
H−cCPC−H	85.5%	14.5%	38.6% (s, 7.7%; p, 92.3%)	61.4% (s, 21.1%; p, 78.9%)	100%
H−cCAsC−H	88.9%	11.1%	38.4% (s, 5.9%; p, 94.1%)	61.6% (s, 19.6%; p, 80.4%)	100%

bond orbital (NBO) [33] analysis are collected in Table 7, from which we can clearly know that the single electron in each H−*c*CXC−H (X = N, P, and As) radical occupies a pure p orbital of X atom. The lone-paired electrons reside in a hybridized orbital, in which the weight of the s orbital of the X atom is more than that in the σ_{XC} orbitals. Of course, we can also realize the fact from Table 7 that H−*c*CPC−H is more homologous in the constitution of molecular orbitals with H−*c*CAsC−H than with H−*c*CNC−H. A visual picture for the orbital nature from the NBO computations is shown as

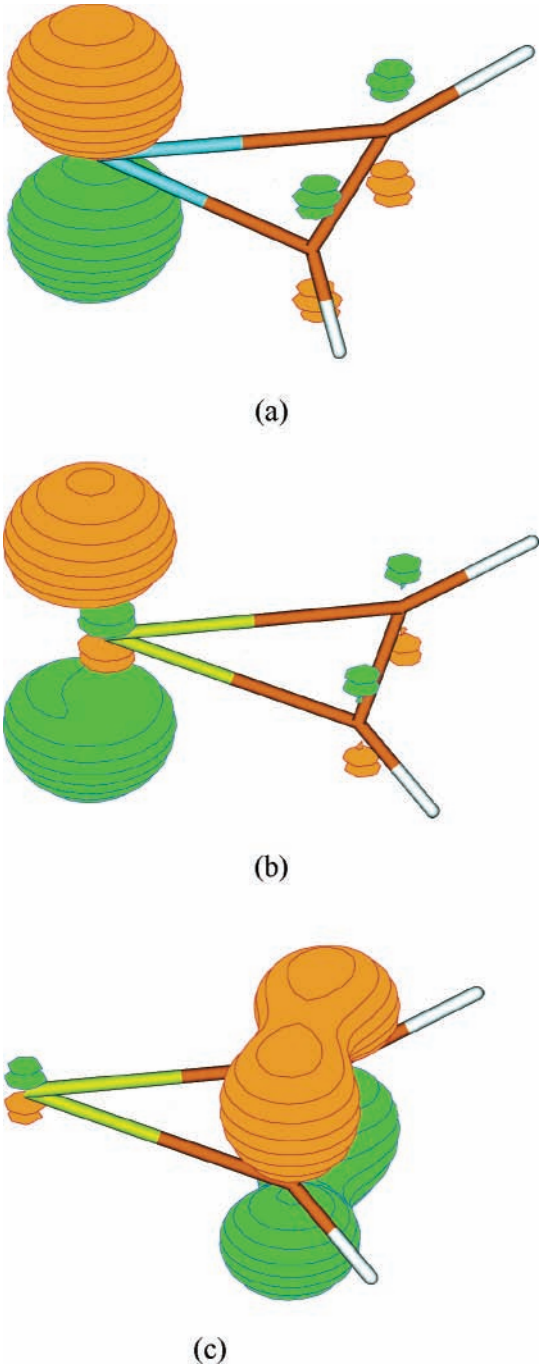

Figure 5. Pictures of orbitals occupied by a single electron ((a) for H−cCNC−H and (b) for H−cCPC−H and H−cCAsC−H) and by π_{CC} bonding electrons ((c) for H−cCNC−H, H−cCPC−H, and H−cCAsC−H).

TABLE 8: Predicted Structural Parameters and Spin Densities of CCR Radicals at the UB3LYP/6-311++G(d,p) Level of Theory

species	bond lengths r_{CC}	bond lengths r_{CX}[a]	dihedral angle ∠HCXH	spin densities *β*-C	spin densities α-C	spin densities X[a]
CCH	1.203			1.01	−0.04	0.03
CCCl	1.275			0.51	0.35	0.14
$CCCF_3$	1.201	1.466		1.17	−0.19	0.02
CCOH	1.284			0.45	0.41	0.15
$CCNH_2$	1.280	1.304	180.0	0.51	0.25	0.26
$CCPH_2$	1.276	1.697	108.2	0.41	0.24	0.31
$CCAsH_2$	1.272	1.850	99.8	0.44	0.34	0.15

[a] X represents the substituent atom or the atom of the substituent group connecting directly with carbon (α-C) atom.

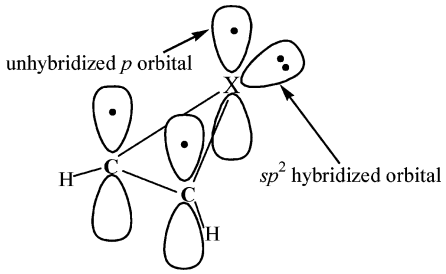

3.3.4. Isomer $CCPH_2$. Isomer $CCPH_2$ **8** with $^2A'$ electronic state possesses C_S symmetry and two identical hydrogen atoms. Its CC bond value (1.276 Å) lies between the normal C=C (1.329 Å in ethylene) and C≡C (1.199 Å in acetylene) bond lengths. Species **8** has a 1.696 Å CP bond, which should be regard as an intermediate between single and double bonds. The spin densities of *β*-C, α-C, and P atoms are 0.41, 0.24, and 0.31 e, respectively, which indicates that the single unpaired electron is highly delocalized among the phosphorus atom and two carbon atoms. Thus, isomer **8** can be viewed as a resonant structure between three extreme forms

$$\dot{C}\equiv C-\ddot{P}H_2 \leftrightarrow :C=\dot{C}-\ddot{P}H_2 \leftrightarrow :C=C=\dot{P}H_2$$

although somewhat higher spin density on the *β*-C atom suggests a slightly greater contribution of the canonical structure $\dot{C}\equiv C-PH_2$. The nitrogen and arsenic analogues of $CCPH_2$, $CCNH_2$, and $CCAsH_2$, exhibit features similar to those of species $CCPH_2$ estimated from the bond lengths and spin single electron distribution shown in Table 8.

In $CCNH_2$, $CCPH_2$, and $CCAsH_2$ radicals, there are almost the same CC bond lengths (less than 0.008 Å from one another, as presented in Table 8), demonstrating a very analogical C−C bonding nature, which can also be noticed from the respective spin densities of the corresponding atoms. A remarkable differentiation among $CCNH_2$, $CCPH_2$, and $CCAsH_2$ radicals should be focused on their geometric structures. As listed in Table 8, the $CCPH_2$ and $CCAsH_2$ radicals are found to be

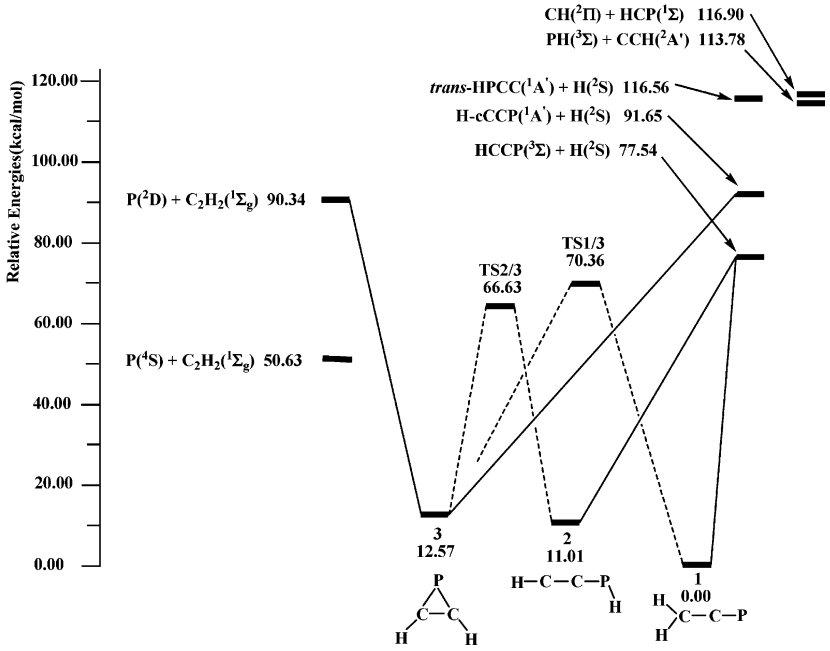

Figure 6. Schematic energy diagram for the reaction $P(^2D) + C_2H_2(^1\Sigma_g)$ at the UCCSD(T)/6-311++G(2df,2p)//UB3LYP/6-311++G(d,p) level with zero-point vibrational energy correction. The energy level of the CH_2CP radical is set to be zero.

nonplanar species with HCXH dihedral angles of 108.2 and 99.8°, respectively, but for $CCNH_2$ it is 180.0°, suggesting a planar configuration. It is interesting to note that the C−C bond lengths in several CCX molecules are found in the range of 1.27−1.29 Å depending on different substituents (X = Cl−, OH−, NH_2−, PH_2−, AsH_2−), which are apparently longer than 1.203 Å in CCH species, as presented in Table 8. The above results can be considered to come from effective orbital conjugation between π_{CC} and substituents X (X = Cl−, OH−, NH_2−, PH_2−, AsH_2−). Furthermore, the results can be also affected by the spin single electron delocalization effect if considering 0.41−0.51 spin density distribution on the β-C atoms of CCX (X = Cl−, OH−, NH_2−, PH_2−, AsH_2−) molecules and spin density of 1.01 on the terminal carbon atom of CCH molecule. If no conjugation effect exists in a radical system, the single or lone-paired electrons cannot be delocalized along the molecular chain, and the system cannot be stabilized. For example, in the $CCCF_3$ system with the stronger CF bonds and with the electron withdrawing $-CF_3$ group, there is no spin single electron delocalization found based on the spin density distribution (β-C, 1.17 e) shown in Table 8. Furthermore, the CC bond length 1.201 Å in $CCCF_3$ is very close to the corresponding bond distance value (1.203 Å) in reference molecule HCC, indicating that no obvious $\pi-\pi$ or $\sigma-\pi$ conjugation effect exists between $-CF_3$ and CC.

As mentioned above, the radical $CCPH_2$ can rearrange into isomers **2** and **5** via directly H-shift and ring-close pathways, respectively, with higher reaction barriers, suggesting it to be a stable radical at normal temperature, although it lies 65.36 kcal/mol above the thermodynamically most stable species CH_2CP. On the basis of the discussed structural features, the stability can be believed to come from the extended delocalization effect of unpaired and lone-paired electrons along the molecular chain, which can be adequately reflected from spin density distribution. Considering the higher stability of HCC[19] and CCOH[34,35] and the predicted structural nature and kinetic stability of $CCPH_2$, we suggest that the molecule $CCPH_2$ may be experimentally observable.

3.4. An Implication for Possible Experiments. For the [C_2, H_2, N] system, cyclic isomer H−cCNC−H, the nitrogen analogue of H−cCPC−H (**3**), has been experimentally confirmed to exist as an intermediate product in the reaction of excited nitrogen atoms with acetylene.[23,26,27] Then, it is reasonable to suggest species H−cCPC−H **3**, in view of its higher kinetic stability, to be an excellent candidate for experimental observation. Therefore, it is necessary to discuss the possibility of formation of species **3** in the reaction between excited phosphorus atoms and acetylene. A schematic reaction diagram with reactants, intermediates, products, and transition states is shown in Figure 6. From the figure we can easily know that the energy of excited-state $P(^2D)$ is 39.71 kcal/mol above the ground-state $P(^4S)$. On the basis of the structural nature of acetylene and the reaction mechanism of excited nitrogen with acetylene, the most possible reaction pathway of excited phosphorus added to the π bond of acetylene can be estimated to be a direct attack by excited phosphorus on the reactant acetylene to produce a cyclic radical **3**. In the reaction of excited nitrogen atoms with acetylene leading to the formation of three-membered ring H−cCNC−H, the barrier height was calculated to be 2.9 kcal/mol at the PMP4(full,SDTQ)/cc-pVTZ//CASSCF-(7,7)/cc-pVTZ level of theory with zero-point energy correction.[26] But unfortunately, for the present reaction system consisting of excited phosphorus atom and acetylene, we did not locate the corresponding reaction transition state despite of a lot of expensive work. To confirm it to be a zero-barrier reaction, a potential energy surface scanning technology embedded in the Gaussian98 package was applied in the present work. At the B3LYP/6-311++G(d,p) level of theory, the interaction energy between excited phosphorus and acetylene was calculated as a function of both the distance, adopting the length of phosphorus atom and the equilibrium position of phosphorus in the radical **3**, and the orientation angle, as displayed in Figure 7 in company with the calculated results. In the optimizations, the distances of P_0X and CX and the angle CXP_0 of 90° were frozen, while the remaining bond parameters were optimized.

From the computed results presented in Figure 7, it can be easily noticed that, if total energies are equal to each other for different orientation angles, the P atom is the nearest to the equilibrium position P_0 when the orientation angle θ is zero. Therefore, the approach with orientation angle $\theta = 0$ is

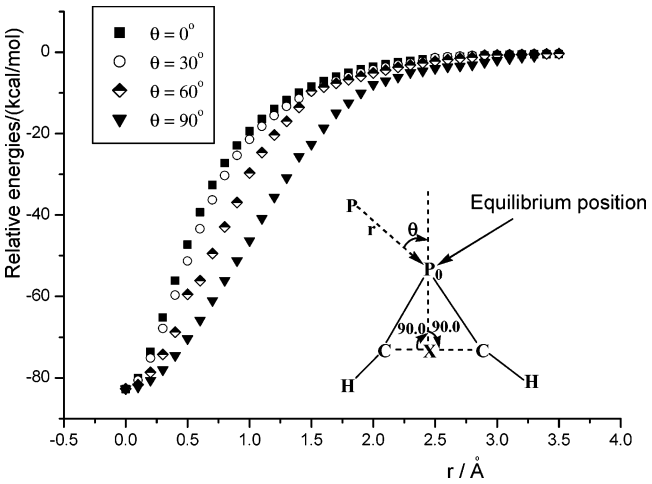

Figure 7. Potential energy curves as a function of the distance between phosphorus atom and the equilibrium position of phosphorus (P_0) in radical **3** at the B3LYP/6-311++G(d,p) level of theory.

energetically the most favorable. The continuously smooth falling in interaction potential from infinite distance to the equilibrium position suggests the approach with $\theta = 0$ to be a zero-barrier process; e.g., the reaction entrance barrier is zero.

There are two important rearrangement reaction pathways and a dissociation channel for the product radical **3** from the reaction of excited phosphorus atoms with acetylene. The rearrangement reactions are two isomerization processes into the intermediates **2** and **1** via two ring-open reactions connected by transition states **TS2/3** and **TS1/3** with 54.06 and 57.79 kcal/mol reaction barrier heights, respectively. The dissociation channel is the direct dissociation of C−H bond of intermediate radical **3** leading to the formation of H−cCCP(^{1}A′) and H(^{2}S) with a dissociation energy of 79.08 kcal/mol. On the basis of the required energies for the three pathways, we can know that the isomerization processes **3** → **2** and **3** → **1** is more favorable than the direct H-loss dissociation channel. Therefore, the isomers **2** and **1** can form from intermediate **3**. For species **2** and **1**, the most favorable dissociation reaction channel is the direct dissociation which leads to the loss of a hydrogen atom and the formation of HCCP($^3\Sigma$), a well studied potential interstellar molecule.[8,36,37] And thus, one can see that the HCCP-($^3\Sigma$) and H−cCCP (^{1}A′) may be detectable in a sophisticated experiment. In these reactions, because of higher isomerization barriers and direct dissociation energies, we may be able to isolate or observe the intermediates CH_2CP (**1**), H−cCPC−H (**3**), and HCCPH (**2**) provided that precise experimental conditions are used. The present computational results about the reaction of excited phosphorus with acetylene are found to be very similar to the mechanism of reaction between excited N(^{2}D) and acetylene.

4. Summary and Conclusions

A detailed doublet potential energy surface of the [C_2, H_2, P] system including eight minimum isomers and 10 transition states is constructed at the UB3LYP/6-311++G(d,p) and UCCSD(T)/6-311++G(2df,2p) (single-point) levels of theory. The global minimum is found to be the chainlike isomer CH_2-CP **1**, followed by the kinetically stable isomers HCCPH (**2**), H−cCPC−H (**3**), and $CCPH_2$ (**8**) at 11.01, 12.57, and 65.36 kcal/mol, respectively. These isomers may be detected at extra low pressures and temperatures. The structural and bonding properties of relevant species are analyzed.

For the isomer CH_2CP, the C−C bond is a slightly weak double bond, while the C−P bond is a somewhat stronger double bond. In two resonance structures of CH_2CP, the component of $H_2C{=}C{=}P\bullet$ structure should be slight more than $H_2C\bullet{-}C{\equiv}\ddot{P}$ form based on the calculated bond lengths and spin density distribution, and the results are in qualitative agreement with the available microwave spectroscopic experiments. The computed results about bonding features and single electron density distribution suggest that the species HCCPH should be viewed as a resonance structure between H−C≡C −Ṗ−H and H−Ċ=C=P−H. The only kinetically stable cyclic species H−cCPC−H was found to possess a CC double bond and two CP single bonds with the unpaired electron residing on the P atom, and thus, indicating evident single electron localization effect. Furthermore, on the basis of the discussed structural features, the stability of radical $CCPH_2$ was believed to come from the extended delocalization effect of unpaired and lone-paired electrons along the molecular chain.

The present work also found that in the reaction P (^{2}D) + C_2H_2($^1\Sigma_g$) the detection of HCCP($^3\Sigma$) is possible according to the provided thermodynamic profiles. The reaction was also believed to be available for the possible experimental observation of intermediate radicals CH_2CP, H−cCPC−H, and HCCPH.

Acknowledgment. This work is supported by the National Natural Science Foundation of China (No. 20431030, 20301006), the Science Foundation for Young Scholar of Heilongjiang University (Q200242), and the Research Project of Department of Education of Heilongjiang Province (10551234).

References and Notes

(1) Markovski, L. N.; Romanenko, V. D. *Tetrahedron* **1988**, *45*, 6019.
(2) Nixon, J. F. *Chem. Rev.* **1988**, *88*, 1327.
(3) Regitz, M. *Chem. Rev.* **1990**, *90*, 191.
(4) Regitz, M. *J. Heterocyclic Chem.* **1994**, *31*, 663.
(5) Ram, R. S.; Bernath, P. F. *J. Mol. Spectrosc.* **1987**, *122*, 282.
(6) Saito, S.; Yamamoto, S.; Kawaguchi, K.; Ohishi, M.; Ishikawa, S.; Kaifu, N. *Astrophys. J. Lett.* **1989**, *341*, 1114.
(7) Klein, H.; Klisch, E.; Winnewisser, G.; Königshofen, A.; Hahn, J. *Z. Naturforsch., A: Phys. Sci.* **1999**, *54a*, 187.
(8) Ahmad, I. K.; Ozeki, H.; Saito, S. *J. Chem. Phys.* **1997**, *107*, 1301.
(9) Guélin, M.; Cernicharo, J.; Paubert, G.; Turner, B. E. *Astron. Astrophys.* **1990**, *230*, L9.
(10) Gonbeau, D.; Pfister-Guillouzo, G. *Nouv. Chim.* **1985**, *9*, 71.
(11) Ahmad, I. K.; Ozeki, H.; Saito, S.; Botschwina, P. *J. Chem. Phys.* **1998**, *109*, 4252.
(12) Ozeki, H.; Habara, H.; Ahmad, I. K.; Saito, S.; Yamamoto, S. *J. Chem. Phys.* **2002**, *117*, 5670.
(13) Gutsev, G. L.; Adamowicz, L. *Chem. Phys. Lett.* **1995**, *246*, 245.
(14) Saito, S.; Yamamoto, S. *J. Chem. Phys.* **1997**, *107*, 1732.
(15) Frisch, M. J.; Trucks, G. W.; Schlegel, H. B.; Scuseria, G. E.; Robb, M. A.; Cheeseman, J. R.; Zakrzewski, V. G.; Montgomery, J. A., Jr.; Stratmann, R. E.; Burant, J. C.; Dapprich, S.; Millam, J. M.; Daniels, A. D.; Kudin, K. N.; Strain, M. C.; Farkas, O.; Tomasi, J.; Barone, V.; Cossi, M.; Cammi, R.; Mennucci, B.; Pomelli, C.; Adamo, C.; Clifford, S.; Ochterski, J.; Petersson, G. A.; Ayala, P. Y.; Cui, Q.; Morokuma, K.; Malick, D. K.; Rabuck, A. D.; Raghavachari, K.; Foresman, J. B.; Cioslowski, J.; Ortiz, J. V.; Stefanov, B. B.; Liu, G.; Liashenko, A.; Piskorz, P.; Komaromi, I.; Gomperts, R.; Martin, R. L.; Fox, D. J.; Keith, T.; Al-Laham, M. A.; Peng, C. Y.; Nanayakkara, A.; Gonzalez, C.; Challacombe, M.; Gill, P. M. W.; Johnson, B. G.; Chen, W.; Wong, M. W.; Andres, J. L.; Head-Gordon, M.; Replogle, E. S.; Pople, J. A. *Gaussian 98*, revision A.11.2. Gaussian, Inc.: Pittsburgh, PA, 1998.
(16) Lee, C.; Yang, W.; Parr, R. G. *Phys. Rev. B* **1988**, *37*, 785.
(17) Stevenes, P. J.; Devlin, F. J.; Chabalowski, C. F.; Frisch, M. J. *J. Phys. Chem.* **1994**, *98*, 11623.
(18) Becke, A. D. *J. Chem. Phys.* **1993**, *98*, 1372.
(19) Scuseria, G. E.; Janssen, C. L.; Schaefer, H. F., III. *J. Chem. Phys.* **1988**, *89*, 7382.
(20) Scuseria, G. E.; Schaefer, H. F., III. *J. Chem. Phys.* **1989**, *90*, 3700.
(21) Gonzalez, C.; Schlegel, H. B. *J. Chem. Phys.* **1989**, *90*, 2154.
(22) Gonzalez, C.; Schlegel, H. B. *J. Phys. Chem.* **1990**, *94*, 5523.

(23) Balucani, N.; Alagia, M.; Cartechini, L.; Casavecchia, P.; Volpi, G. G.; Sato, K.; Takayanagi, T.; Kurosaki, Y. *J. Am. Chem. Soc.* **2000**, *122*, 4443.

(24) Curtiss, L. A.; Raghavachari, K.; Trucks, G. W.; Pople, J. A. *J. Chem. Phys.* **1991**, *94*, 7221.

(25) Curtiss, L. A.; Raghavachari, K.; Trucks, G. W.; Pople, J. A. *J. Chem. Phys.* **1993**, *98*, 1293.

(26) Takayanagi, T.; Kurosaki, Y. *J. Phys. Chem. A* **1998**, *102*, 6251.

(27) Holmes, J. L.; Mayer, P. M. *J. Phys. Chem.* **1995**, *99*, 1366.

(28) Glukhovtsev, M. N.; Laiter, S.; Pross, A. *J. Phys. Chem.* **1996**, *100*, 17801.

(29) Kass, S. R.; Merrill, G. N. *J. Am. Chem. Soc.* **1997**, *119*, 12322.

(30) Mayer, P. M.; Taylor, M. S.; Wong, M. W.; Radom, L. *J. Phys. Chem. A* **1998**, *102*, 7074.

(31) Forney, D.; Jacox, M. E.; Thompson, W. E. *J. Mol. Spectrosc.* **1995**, *170*, 178.

(32) G. Schaftenaar, *Molden*, CAOS/CAMM Center Nijmegen: Toernooiveld, Nijmegen, The Netherlands, 1991.

(33) Glendening, E. D.; Badenhoop, J. K.; Reed, A. E.; Carpenter, J. E.; Bohmann, J. A.; Morales, C. M.; Weinhold, F. *NBO*, version 5.0; Theoretical Chemistry Institute, University of Wisconsin: Madison, WI, 2001.

(34) Venkatasubramanian, R.; Krishnamachari, S. L. N. G. *Indian J. Pure Appl. Phys.* **1991**, *29*, 697.

(35) Yamaguchi, Y.; Rienstra-Kiracofe, J. C.; Stephens, J. C.; Schaefer, H. F., III. *Chem. Phys. Lett.* **1998**, *291*, 509.

(36) Shao, G. Q.; Fang, W. H. *Chem. Phys. Lett.* **1998**, *290*, 193.

(37) Ding, Y. H.; Li, Z. S.; Tao, Y. G.; Huang, X. R.; Sun, C. C. *Theor. Chem. Acc.* **2002**, *107*, 253.